NURETH14-100

TRIPARTITE MASS TRANSFER MODEL: DEVELOPMENT, IMPLEMENTATION IN DYVRO, VERIFICATION AND VALIDATION

T. Neuhaus[1] and A. Schaffrath[1]
[1] TÜV NORD SysTec GmbH & Co. KG, Hamburg, Germany

Abstract

The calculation of condensation induced water hammer (CIWH) resulting from the contact of steam and sub-cooled water, is still a sophisticated challenge because of time-dependent condensation, highly transient flow phenomena and the change of flow pattern. In this paper a tripartite mass transfer (TMT) model that accounts for vaporization due to flashing, condensation due to isentropic decompression and direct contact condensation at the phase interface is presented. The TMT model shall be considered as a frame for sub-models which may be arranged for the above phenomena. For contact condensation a simplified approach has been applied taking into account a constant heat transfer coefficient and a basic approach for the calculation of the interface area. The TMT model has been implemented in the one-dimensional two-phase pressure surge code DYVRO mod 3. A verification and validation procedure was performed based on experiments at test facilities in Oberhausen (PPP), Rossendorf (CWHTF) and Budapest (PMK-2). The computational results of the column rejoining experiments at PPP and CWHTF show better agreement to experimental data in comparison to the application of an equilibrium model. Especially the relatively gentle pressure and temperature increase, when the steam bubble collapses respectively when the steam bubble is compressed, can be captured better. Concerning the condensation induced water hammer experiments after steam/water counter-flow in a horizontal pipe, which was examined at PMK-2, a parameter study was performed with DYVRO. As initial conditions stratified flow conditions are defined. The phenomenology and the maximum pressure increase could be satisfactorily approximated by DYVRO in combination with the TMT model. In future the direct contact condensation model shall be improved using flow velocity dependent heat transfer coefficients.

Introduction

In pipe systems different types of water hammer may arise which can damage the pipes and the supports. Griffith identified seven mechanisms in the water hammer handbook from 1996 [1] which can lead to severe water hammer:

1. Sub-cooled water with condensing steam in a vertical pipe (water cannon)
2. Steam and water counter-flow in a horizontal pipe (steam/water counter-flow)
3. Pressurized water entering a vertical steam-filled pipe (steam pocket collapse)
4. Hot water entering a low pressure line (low pressure discharge)
5. Steam-propelled water slug (water slug)
6. Rapid valve actuation (valve slam)
7. Filling of a voided line (column rejoining)

For the mechanisms 4 and 5 the condensation is of minor importance. A valve slam (mechanism 6) may lead to column separation downstream the valve, if saturation pressure is reached. In this case the steam temperature approximately equals the water temperature. The subsequent collapse of the steam bubble can satisfyingly be calculated by codes, which use a thermodynamic equilibrium model. For the calculation of mechanism 7 a thermodynamic equilibrium model may also lead to acceptable results. In reference [1] several computer codes are listed which may be able to calculate the water hammer mechanisms 4-7.

For the mechanisms 1-3 the temperature difference between steam and water and the resulting contact condensation plays an important role. For the simulation of these phenomena a code should be applied that can handle thermodynamic non-equilibrium. In [1] it is stated, that the mechanisms 1 to 3 have not been analysed by any computer program. Moreover in [1] the assessment has been made that there is no code capable to calculate these phenomena, except two codes which may calculate the terminal velocity for impact load calculation in case of water hammer mechanism 1 (water cannon).

For the mechanism “steam/water counter-flow” another important effect to be considered is the slugging that occurs, when the relative velocity between the sub-cooled water and the condensing steam is increased. The simulation of this water hammer phenomenon was and still is a challenging subject.

The EU-project WAHALoads (2000-2004) [2] dealt with water hammer loads in nuclear power plants. One outcome of WAHALoads was the computer code WAHA that uses a 6 equation model and a relaxation model for the mass transfer between the phases. This code was used to calculate “steam/water counter-flow”-experiments, which have been performed at the test facility PMK-2 at the institute AEKI-KFKI in Budapest, Hungary. In reference [3] and [4] is shown that WAHA can calculate the slugging satisfactorily. The final statement of the authors however is, that recent numerical models and analyses can forecast, if a condensation induced water hammer (CIWH) event happens in a flow system with great confidence, but the absolute value of the overpressure peak needs further peculiar investigation.

The present paper shall provide a new tripartite mass transfer (TMT) model with which contact condensation is accounted for using Newton’s law of heat transfer. As for the water hammer mechanisms 1-3 the contact condensation is essential for the physical phenomenology, it is expected that a detailed model of the contact condensation may lead to a better agreement with experimental data. Especially for condensation induced water hammer at high initial system pressure that may be heat-transfer limited and not inertially controlled the application of Newton’s law of heat transfer is expected to be more appropriate than the thermodynamic equilibrium model that experientially leads to unrealistic high pressure peaks in this case.

Since water hammer phenomena are accompanied by highly transient pressure fluctuations, which may also lead to other mass transfer phenomena, the presented model also accounts for flashing and isentropic expansion into the two-phase flow regime. Those phenomena are described in the next chapter. The new TMT model shall be considered as a frame for sub-models which may be arranged for the mass transfer phenomena described above in a more or less detailed manner. In the present paper simplified sub-models are chosen in a first step to investigate the potential of the TMT model.

1. Tripartite mass transfer model

Water hammers are usually accompanied by the fast local change of fluid conditions and properties. These transient processes can be regarded as isentropic. The pressure change in a liquid does not lead to an extensive change of the temperature as long as the water does not vaporize. In contrast an isentropic pressurization of vapour results in a noticeable temperature increase. In this case it can be derived from the T-s-diagram that the distance to the saturation line increases (see figure 1).

On the other hand an isentropic depressurization of superheated steam leads to a temperature reduction. If the pressure and the accompanied temperature decrease is big enough, the saturation line is reached. With a further depressurization an expansion into the two-phase regime occurs (see right side of figure 1). Here the temperature decrease is not as strong as in the superheated regime, because the condensation energy must be absorbed from the arising two-phase mixture. This kind of condensation is referred to as isentropic expansion into the two-phase regime.

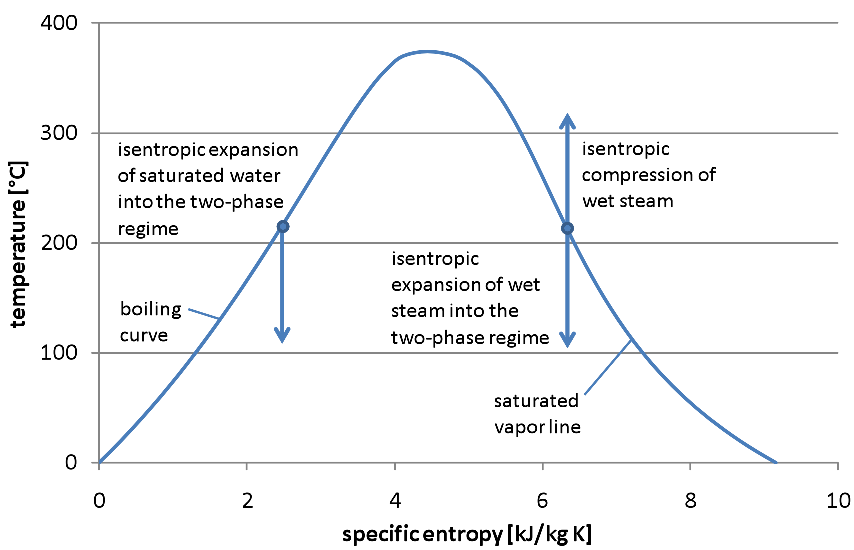

Figure 1 Phase change due to isentropic expansion of saturated water or wet steam.

The effect of contact condensation takes places in a different manner. In this case the phase change is caused by the contact of vapour at the surface of a cold solid or liquid. The condensation energy is emitted to the liquid or solid that is consequently heated up. The contact condensation may occur at constant pressure. This is not possible for the first condensation phenomenon.

Also the vaporization of a liquid may arise due to different physical effects. The isentropic flashing due to a pressure decrease (see left side of figure 1) can be distinguished from the boiling process that occurs at a hot solid surface. For the former the vaporisation energy is taken from the arising two-phase mixture leading to a temperature decrease, for the latter the vaporisation energy is provided by the hot solid.

For the effect of contact condensation and boiling the important parameters are the magnitude of the surface area, the temperature gradient and the heat transfer coefficient. Newton's law of heat transfer is often applied for these processes.

In case of the mass transfer due to isentropic expansion the application of Newton's law is difficult, because it is almost impossible to specify the magnitude of the interface area and the time-dependent alteration of its shape. The flashing process occurs in a seething and bubbling manner, since the magnitude of the interface area is generated that is needed to provide the vaporisation energy.

A further effect that complicates the specification of the interface area is the following: If the vapour, which is generated at a certain stage of a flashing process, is regarded as single phase, a further pressure decrease leads to the generation of small droplets in this vapour phase because of the effect of isentropic expansion into the two-phase regime. This leads to an extension of the interface area. Moreover, the generated droplets must partially vaporize in course of further depressurisation leading to another enlargement of the interface area inside the droplets. The consideration of these effects in a mathematical model is quite challenging and shall not be discovered in this paper.

Instead, for the effect of mass transfer due to isentropic expansion of saturated water or wet steam equilibrium or relaxation models are usually applied that are not based on the interface area between the phases. The latter models calculate the mass transfer in dependence of the deviation of the actual conditions to equilibrium conditions.

Generally computer codes do not apply mathematical models for all the mass transfer phenomena described above. But certain cases require a sufficient modelling of all these phenomena to obtain reasonable results. Especially in case of the condensation induced water hammer that occurs at steam/water counter-low in horizontal pipes all the effects described above may have an influence:

- The contact condensation of steam at the sub-cooled water is the primary effect that leads to the counter-flow of water and steam, and finally to slugging.
- The slugging results in the isolation of a steam bubble. The pressure decrease in the steam bubble that causes the acceleration of the slug is accompanied by an isentropic expansion in the two-phase regime.
- The resulting water hammer may be reflected leading to expansion waves which induce flashing.

The tripartite mass transfer (TMT) model that is introduced in this paper is especially developed for the calculation of CIWH in horizontal pipes. It accounts for three of the above-mentioned phenomena:

- Flashing,
- Isentropic expansion of vapour into the two-phase regime,
- Contact condensation of vapour at the sub-cooled liquid.

The vaporisation at a hot solid structure or the condensation at a cold solid is not taken into account. For the TMT model it is necessary that the phase energies or temperatures are treated separately. This approach implies that different phase saturation pressures must be taken into account. The following conditions must be fulfilled to initiate a mass transfer:

- Flashing

$$p < p_{S,L}(T_L) \tag{1}$$

- Isentropic expansion of vapour into the two-phase regime

$$p < p_{S,G}(T_G) \tag{2}$$

- Contact condensation of vapour at the sub-cooled liquid

$$T_L < T_G \tag{3}$$

The three sub-models above may be prepared in a more or less detailed manner. The flashing model may account for a deviation of the actual pressure from the saturation pressure of the liquid in terms of a relaxation model or the pressure must not fall below saturation pressure of the liquid (equilibrium). The same can be considered for the isentropic expansion of vapour into the two-phase regime. For the contact condensation sub-model Newton's law of heat transfer is applied. The phase interface area and the heat transfer coefficient can be modelled in different ways. As a first step in this paper the heat transfer coefficient is assumed to be constant and the phase interface area is calculated using the following simplified correlations for stratified flow in a horizontal pipe:

$$A_i = \alpha\, D\, dz \qquad \alpha \le 0.5 \tag{4}$$

$$A_i = (1-\alpha) D\, dz \qquad \alpha > 0.5 \tag{5}$$

In future the direct contact condensation model shall be improved using flow velocity dependent heat transfer coefficients. In this paper a sensitivity study regarding a constant heat transfer coefficient is performed.

The TMT model has been implemented in the pressure surge code DYVRO mod. 3 (**Dy**namisches **V**erhalten von **Ro**hrleitungsströmungen), that was developed to calculate one-dimensional, transient, one- or two-phase flow processes in pipe systems. DYVRO - like the system codes RELAP5 and ATHLET or the pressure surge code WAHA - solves a system of six partial differential equations that represent conservation equations for mass, momentum and energy. As an option a 5-equation-model is available, in that same phase velocities are assumed, i.e. one momentum balance for both phases is arranged. For a detailed description of DYVRO please refer to reference [5].

2. Verification and validation procedure

In this chapter the verification and validation procedure of the TMT model is described. The verification was performed by the calculation of the contact condensation of steam at sub-cooled water in a defined closed volume, the validation by the calculation of experiments in the following test rigs:

- Cold Water Hammer Test Facility CWHTF at Forschungszentrum Dresden Rossendorf, Germany [6]

- Pilot Plant Pipework PPP at Fraunhofer UMSICHT, Oberhausen, Germany [7]
- PMK-2 at KFKI-AEKI Budapest, Hungary [8].

Simulation results that are obtained with a thermodynamic equilibrium model are used for comparison in case of momentum driven water hammer events like column rejoining scenarios.

2.1 Contact condensation of steam at sub-cooled water in a defined closed volume

This theoretical test case shall give further insight in the condensation process of a steam bubble that is trapped by cold water. It consists of a pipe segment of 1 m length with a diameter of 100 mm that is closed at both ends. Initially the pipe segment is filled with stagnant water at 20 °C and steam at 200 °C, the void fraction is 0.9, the pressure 0.5 MPa. At the beginning the steam is in a superheated condition. In reality a layer of saturated water would evolve at the interface. In the test case this effect is suppressed by setting the heat transfer coefficient to a constant value of 50 kW/(m² K).

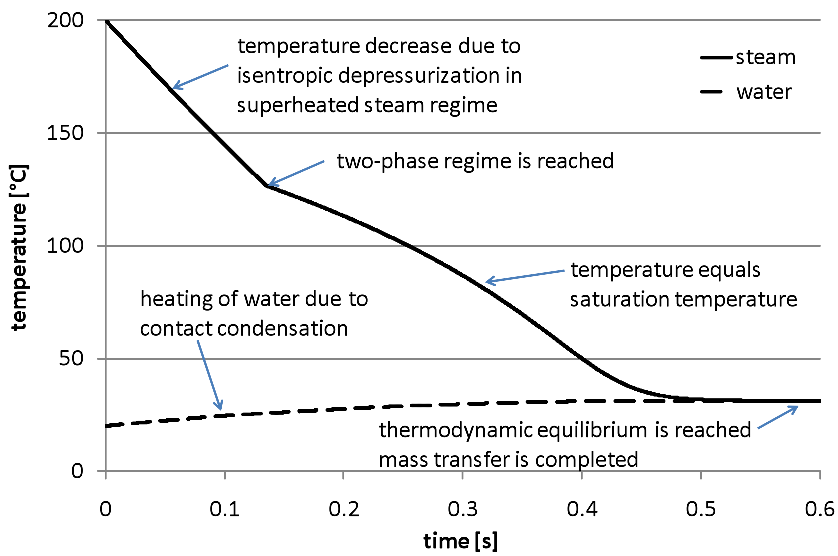

Figure 2 Calculated phase temperatures for the first theoretical test case.

The condensation starts initially due to the contact of hot steam at cold water. The time-dependent temperature is depicted in figure 2. At this stage the condensation energy is completely transferred to the water. Due to the isentropic pressure decrease the superheated steam cools down. When the pressure reaches saturation pressure of the steam at 0.13 s, the isentropic expansion into the two-phase regime takes effect and droplets are generated in the steam. The temperature gradient decreases, because the condensation energy is partly given to the steam/droplet mixture. At this stage the steam temperature equals the saturation temperature. After about 0.5 s thermodynamic equilibrium is reached.

2.2 CWHTF at Forschungszentrum Dresden Rossendorf, Germany

The schematic of the Cold Water Hammer Test Facility (CWHTF) at Helmholzzentrum (former Forschungszentrum) Dresden Rossendorf is shown in figure 3. It consists of a tank, a pipe (inner diameter 0.207 m, length 3.3 m) that has a vertical and a horizontal section, two 90°-bends and a

Eln
Del
Dat

fast opening valve in the horizontal section at a distance of 0.8 m from the tank. The opening time can be varied between 0.02 and 0.5 s by changing the pre-stress of the springs.

For the experiment that was chosen for validation the tank and pipe are filled with water at a temperature of 21 °C. In the beginning the valve is closed and the pressure in the tank is 0.1 MPa.

The pipe section between the closed end and the valve is depressurized so that saturation conditions are reached and a vapour bubble is generated. The volume filled with steam at the closed end has a length of 0.155 m. The pressure at the phase interface near the closed end is 2.9 kPa. The test starts with the rapid opening of the valve, however the exact opening time of the valve is not documented in [3]. The steam bubble collapses 112 ms after the start of the valve opening leading to a pressure surge of 2.5 MPa (see figure 4). The high-frequency pressure oscillations during the high pressure domain probably result from fluid-structure-interaction. This effect is not taken into account in the simulations.

A first parameter study was performed to investigate the influence of the valve opening time (100, 150, 200 ms) on the pressure history. For these calculations the thermodynamic equilibrium model was applied. In all cases the bubble collapse led to a sharp pressure increase up to 3.5 MPa as shown in figure 4. The valve opening time however had an influence on the moment, when the bubble collapse occurred. A value of 150 ms was chosen for further calculations.

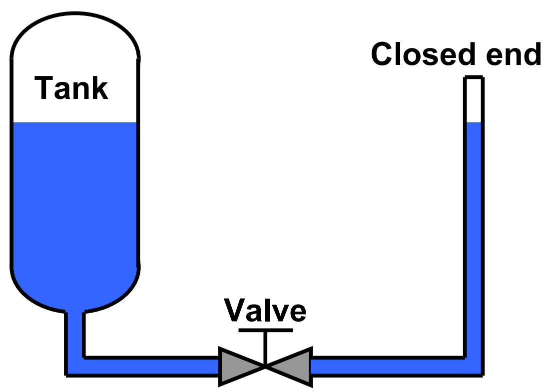

Figure 3 DYVRO pipe model for the PMK-2 test facility.

Due to the discrepancy between experimental data and computational results with the thermodynamic equilibrium model, it was assumed in earlier papers [3, 5] that air may have initially been in the steam phase that damped the pressure surge. But with the assumption of air the pressure gradient in these references was not calculated steep enough. As shown below, reasonable results may also be obtained without assuming air in the steam bubble.

In figure 4 results of simulations are depicted, which were performed with a thermodynamic equilibrium model and the TMT model with different heat transfer coefficients. Applying the TMT model the steam does not condense in the beginning, since the phase temperatures are equal. Due to the acceleration of the water in the direction of the closed pipe end the steam is compressed and therefore heated up. Because of the temperature difference between steam and water the mass transfer due to contact condensation starts to take effect. In the experiment the heat transfer coefficient hc should be relatively low, because presumably the turbulence at the phase interface is minor and a layer of saturated water forms at the phase interface. In the calculation hc it is set to 0, 2 and 10 kW/(m² K).

A value of 0 kW/(m² K) implies that no condensation is calculated at all during the steam compression. The steam acts like a non-condensable gas. For this case the pressure gradient is not calculated steep enough. This approach and the thermodynamic equilibrium model are extreme cases, which represent no condensation and infinitely fast condensation.

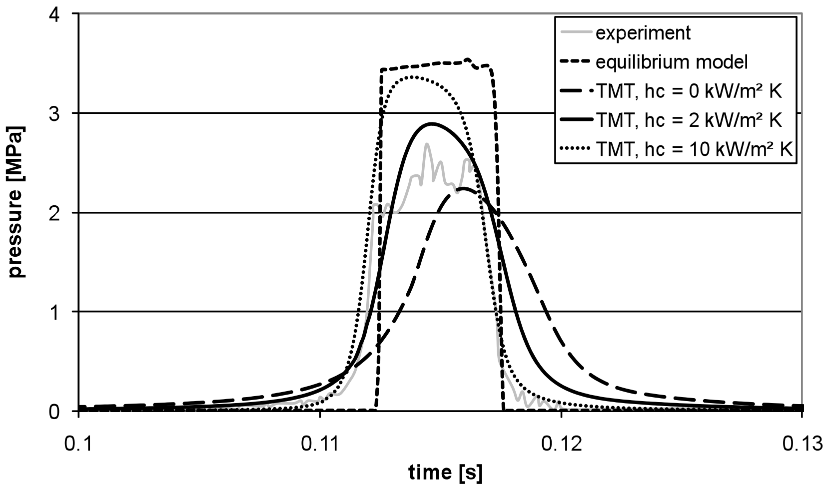

Figure 4 Calculated pressure histories for the CWHTF experiment with varying heat transfer coefficients hc applying the tripartite mass transfer TMT model.

The pressure gradient can be reproduced well with a heat transfer coefficient of 10 kW/(m² K). However, in this case the pressure amplitude is calculated too high. This discrepancy may result from the fluid-structure interaction that affects the pressure evolution in the experiment, but has not been taken into account in the model.

2.3 PPP at Fraunhofer UMSICHT, Oberhausen, Germany

At the PPP test facility water hammers have been researched, which occurred due to column separation and rejoining downstream a fast closing valve. For this paper the experiment 307 was chosen for validation. A detailed description of the experimental apparatus and the experiment can be found in [7]. In figure 5 the geometrical data, the DYVRO pipe model and the position of the pressure transducer P03 is depicted. The experiment starts with a fast valve closure at a water velocity of 3 m/s. The initial pressure is about 1 MPa and the temperature 120 °C.

In figure 6 the measured and calculated pressure is depicted. Calculations were performed applying a thermodynamic equilibrium model and the TMT model with two different heat transfer coefficients. As described above, a value of 0 kW/(m² K) implies that no condensation is calculated during the steam compression.

With the thermodynamic equilibrium model the typical sharp pressure increase is calculated when the steam bubble collapses. The amplitude of the pressure surge is captured well. With the application of the TMT model and a heat transfer coefficient of 0 kW/(m² K) the pressure gradient is calculated too gently and the amplitude too low.

Best results can be obtained with heat transfer coefficients between 50 and 100 kW/(m² K). Here the gradient of the pressure rise and also the amplitude can be reproduced. The high frequency pressure oscillations on the pressure plateau in the experimental data result from fluid-structure-interaction as described in reference [9]. This phenomenon was not taken into account in the simulations.

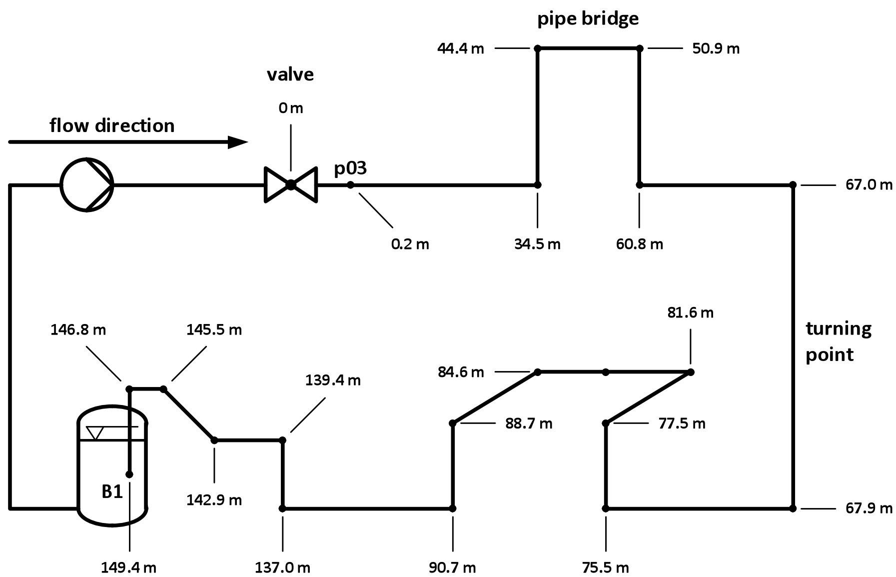

Figure 5 DYVRO pipe model for the PPP test facility at Fraunhofer UMSICHT.

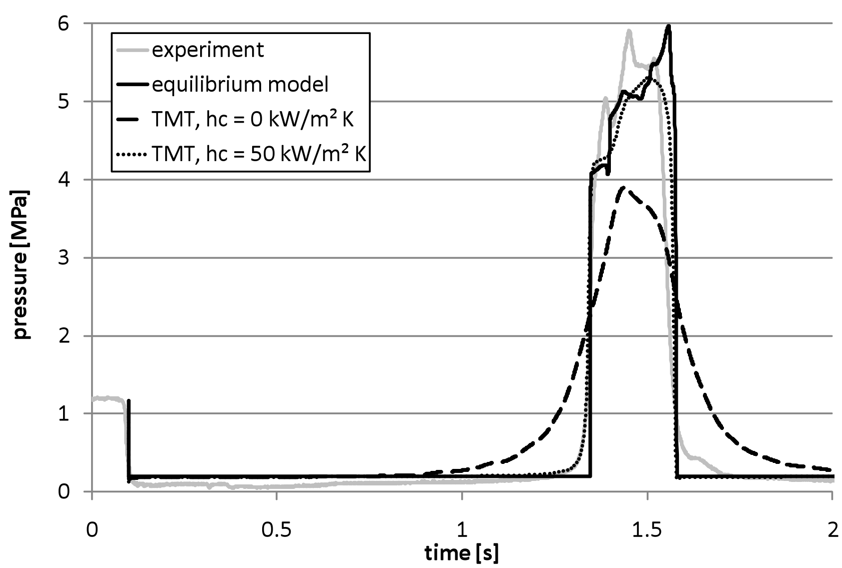

Figure 6 Calculated pressure histories at p03 for the PPP experiment 307.

In figure 7 the measured and calculated temperature increase during the compression of the steam bubble is depicted. At about 1.2 seconds the water bulk reaches the temperature measuring device that is installed 231 mm downstream the fast acting valve so that the temperature of the water (not of the steam) is measured from that point on. Due to the pressure increase the steam is heated up and the steam parameters depart from saturation conditions into the superheated regime. The only reason for condensation then is the contact to the cold water and pipe. Again best results can be obtained with heat transfer coefficients between 50 and 100 kW/(m² K).

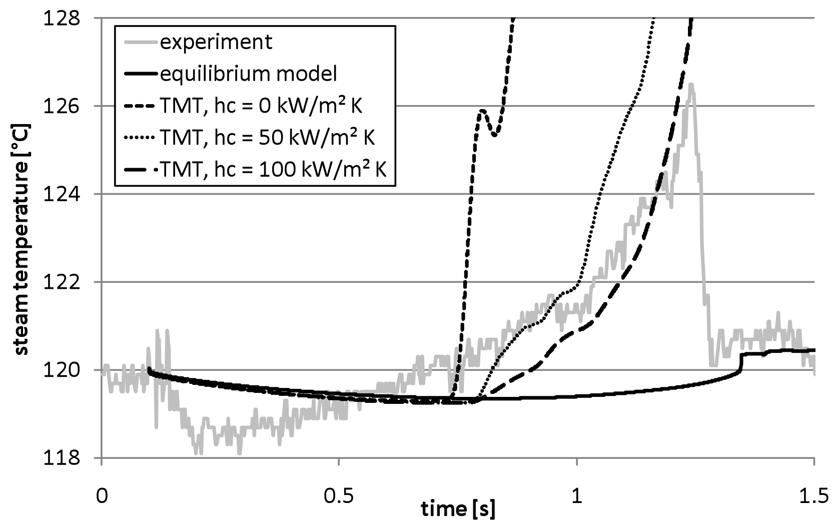

Figure 7 Calculated steam bubble temperature downstream the valve for the PPP experiment 307.

2.4 PMK-2 at KFKI-AEKI, Budapest, Hungary

At the PMK-2 test facility water hammers have been investigated, which occur during steam and water counter-flow in a horizontal pipe. A detailed description of the experimental apparatus can be found in [8]. In figure 8 the geometrical data, the DYVRO pipe model and the position of the pressure transducer P1 is depicted.

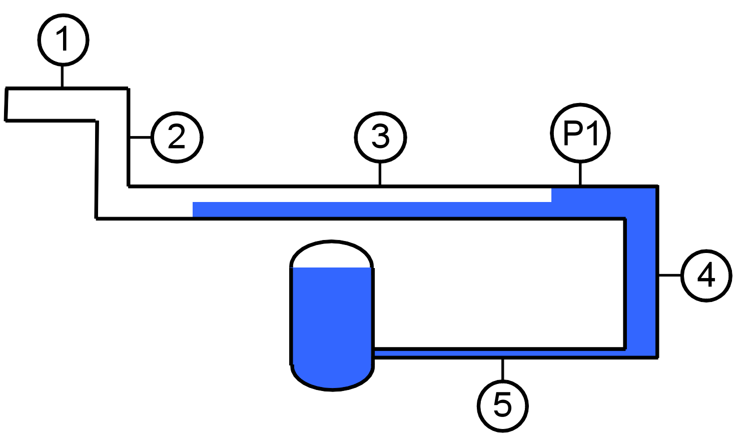

Pipe segment	Pipe length [m]	Pipe diameter [m]
1	0,67	0,073
2	0,39	0,073
3	3,17	0,073
4	0,73	0,073
5	1,94	0,024

Figure 8 DYVRO pipe model for the PMK-2 test facility.

Before the experiment starts, the main steam pipe (segments 1-4) is isolated from the steam generator and condenser by closing both isolation valves, which are located at the left end from pipe segment 1 and at the bottom of pipe segment 4. Afterwards cold water is injected from the cold water tank via the injection line (segment 5). After the vertical pipe (segment 4) has been filled, the cold water enters the test section from the right. Hereby stratified flow conditions are established followed by a condensation-induced water hammer. Test 20 has been chosen for validation, because it is described in detail in reference [8]. The initial steam pressure is 1.17 MPa, the steam temperature 187 °C and the water temperature 53 °C. The water flow rate was set to 1 kg/s.

Presently DYVRO can either simulate stratified flow conditions by means of a 6 equation model with interfacial pressure term that is needed to calculate the filling process of the horizontal pipe or homogenous flow conditions using a 6 equation model with virtual mass approach. Additionally DYVRO can use a 5 equation model with one momentum balance (one fluid velocity) for the homogenous mixture. The two latter models are needed to calculate the high momentum exchange between the phases that occurs during slugging. The transition between stratified flow conditions and slugging cannot be simulated by DYVRO up to now. For this reason the stratified flow condition is set as initial condition as indicated in figure 8 and for the transient calculation the 5 equation model is used to simulate the slugging properly. In reference [8] the phase distribution of test 20 just before the CIWH is well documented, i.e. the stratified flow regime has a length of about 1.6 m.

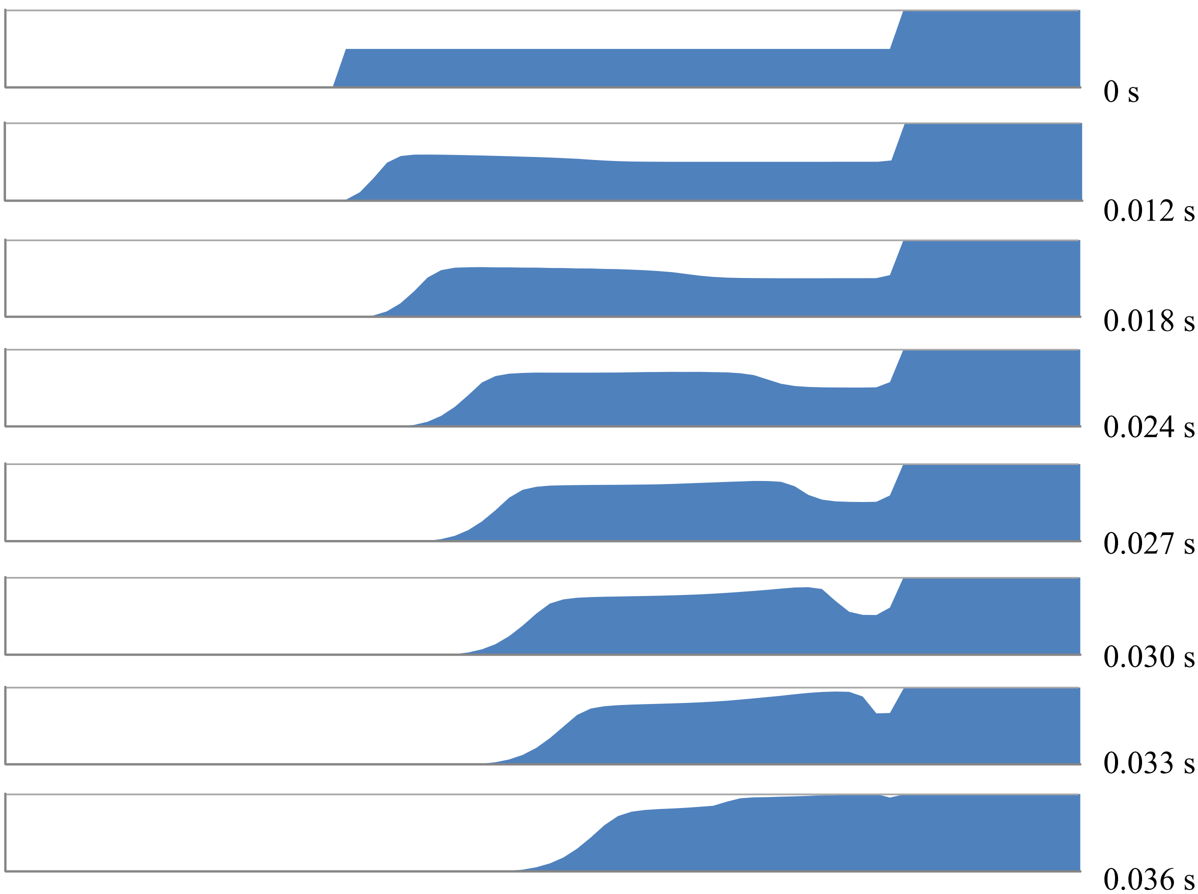

Figure 9 Calculated phase distribution in the test section of PMK-2 for test 20.

Several simulations have been performed. In this paper the results of a run are presented, in which a second order numerical scheme with Minmod flux limiter is used. As described above the application of a 5 equation model with one momentum balance for both phases (steam and water) implicates an infinitely fast momentum exchange between the phases. Calculations performed with two separated momentum balances without the virtual mass approach only led to relatively small water hammers, because the arising slugging could not be simulated properly.

In figure 9 the calculated phase distribution is shown in the test section for different points in time. The contact condensation leads to a steam flow from the left to the right. The biggest relative velocity between the phases is at the left end of the stratified flow regime. Here the slugging is calculated. The slug is accelerated rightward followed by an isolation of a steam bubble that collapses afterwards.

In figure 10 the calculated pressure histories are depicted for heat transfer coefficients of 100 to 150 kW/(m² K). In the simulations two severe water hammers were calculated followed by some moderate pressure fluctuations. This is in accordance to experimental data. The global simulation results are quite sensitive to almost each parameter, but the highest calculated pressure at position P1 is always close to the measured pressure peak of about 13 MPa [8].

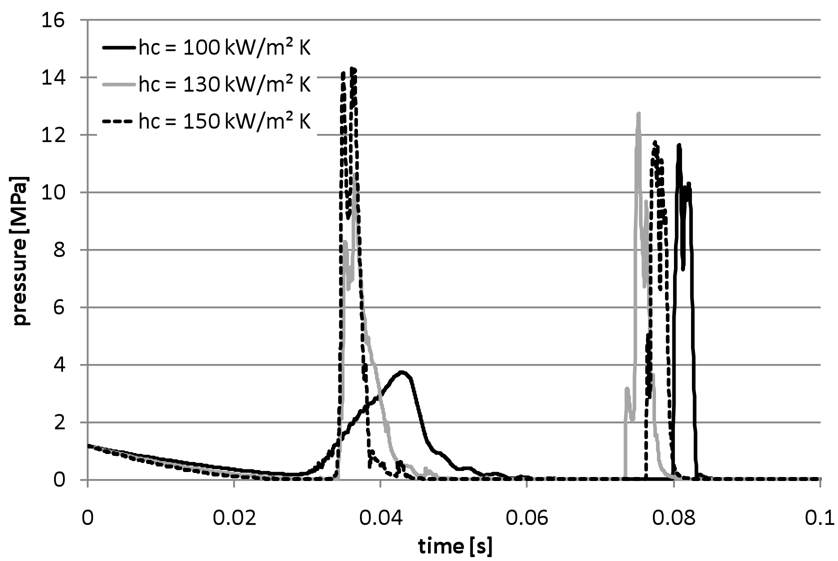

Figure 10 Calculated pressure history at P1 for test 20 of PMK-2 applying the TMT model with different heat transfer coefficients hc.

It shall be noted that the maximum calculated pressure is not at position P1 but in the vertical pipe segment 4. The reason is that the primary water hammer propagates to the right and is reflected almost doubly at the junction to the injection pipe. On the other hand the pressure surge cannot travel to the left into the two-phase regime keeping its primary amplitude. The maximum calculated pressure along the main pipe (segments 1-4) is shown in figure 11.

As described in reference [8] no pressure fluctuations have been measured at positions P2 and P3 during the first experimental stage. This is in accordance to the simulation data.

From figure 11 it can also be derived that the maximum calculated pressure at position P1 would have been different, if the initial phase distribution was set differently for the simulations described above. In case the CIWH had occurred earlier, the calculated pressure at P1 would have been lower, because at this position the two-phase regime would be present and the regime in which the pipe is filled completely with water would not have proceeded so far to the left. The same may be effective for the experiments. In some test runs only minor pressure peaks were detected (tests 10, 13 or 14),

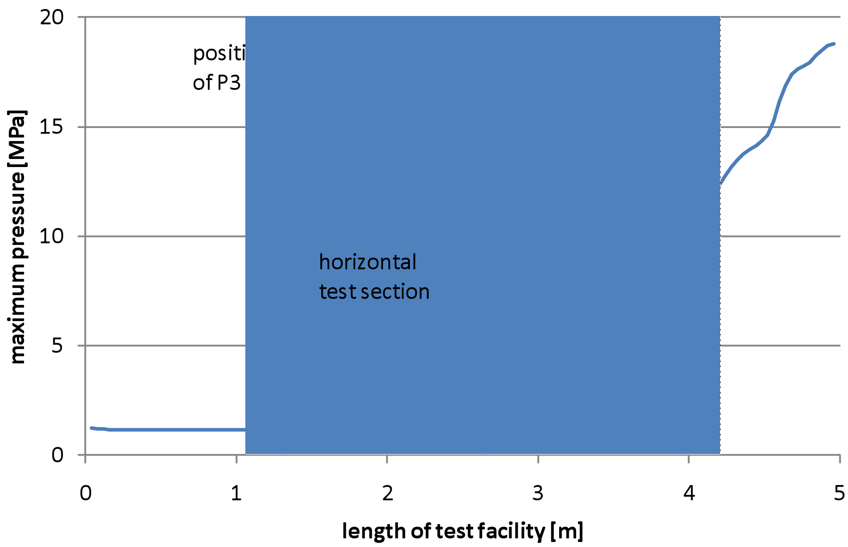

Figure 11 Calculated maximum pressure in the whole test facility for test 20 of PMK-2.

though at similar conditions severe pressure peaks were measured during other test runs. This may be ascribed to the stochastic nature of water hammer during steam/water counter-flow. But one reason could also be that indeed high pressure peaks occurred, but they were not measured due to the effect described above. For this reason validation against other test runs of PMK-2 have not been performed, as the initial phase distribution of experiments other than run 20 is not clear. However, test case 32 was simulated (initial parameters: 4 MPa, water temperature 130 °C), because in this experiment no water hammer occurred at all. In accordance to this only minor pressure fluctuations < 1 MPa were calculated for test run 32.

3. Conclusion

Different mass transfer phenomena may arise during water hammer scenarios. In column separation or blowdown scenarios the pressure falls below the saturation pressure causing vaporization. Relaxation models are capable to calculate these kinds of processes. An increase of the local system pressure, as e.g. in column rejoining scenarios, leads to the condensation of a steam bubble. This process is referred to as “collapse“. This paper shows that in the case of the pressurization of a steam bubble the thermodynamic properties of the steam do not run into the metastable region but into the superheated regime. The basic approach of a relaxation model that calculates the mass transfer in dependence of the deviation of actual metastable conditions from thermodynamic equilibrium conditions may principally not be appropriate. The condensation of the steam bubble is exclusively caused by the contact condensation at the cold water or cold structures for any CIWH scenario. For this physical phenomenon a mass transfer model that is based on Newton’s law of heat transfer seems to be more appropriate. The tripartite mass transfer (TMT) model that is introduced in this paper is capable to account for vaporization due to flashing, condensation due to isentropic decompression and direct contact condensation at the phase interface. The TMT model is essentially a frame for sub-models which may be arranged for these different mass transfer phenomena. The application of simplified sub-models already leads to satisfactory results as shown by means of the validation on the basis of two column rejoining experiments and one steam/water counter-flow experiment. The potential of the TMT model is supposed to be high, especially for the calculation of other water hammer mechanisms, for which the temperature difference between steam and water and the resulting contact condensation plays an important role, i.e. water cannon and steam pocket collapse. Especially for condensation induced water hammer at high initial system pressure that may be heat-transfer limited and not inertially controlled the application of the TMT model is expected to be more appropriate than the thermodynamic equilibrium model that experientially leads to unrealistic high pressure peaks for those cases. In future the direct contact condensation model shall be improved using flow velocity dependent heat transfer coefficients. Especially for the water hammer mechanism appearing during steam/water counter-flow in horizontal pipes it is not sufficient just to apply a detailed mass transfer model. Additionally it is necessary to build up a model that can capture the whole water hammer process, i.e. filling, stratifying, slugging and steam bubble collapsing.

4. References

[1] Electric Power Research Institute, "Water hammer handbook for nuclear plant engineers and operators", EPRI TR-106438, 1996.

[2] M. Giot , H. M. Prasser, A. Dudlik, G. Ezsol, J. Jeschke, H. Lemonnier, I. Tiselj, F. Castrillo, W. Van Hove, R. Perezagua, S. Potapov, "Two-phase flow water hammer transients and induced loads on materials and structures of nuclear power plants (WAHALOADS) ", FISA-2003 EU Research in Reactor Safety, Luxembourg, November 2003.

[3] J. Gale, I. Tiselj, "WAHA (Water Hammer) computer code", The Practical Application of Surge Analysis for Design and Operation, 9th International Conference on Pressure Surges, Chester, UK, 24-26 March 2004, Vol. 2, pp. 619-632.

[4] I. F. Barna, A. R. Imre, G. Baranyai, G. Ézsöl, "Experimental and theoretical study of steam condensation induced water hammer phenomena", *Nuclear Engineering and Design* 240, 2010, pp. 146–150.

[5] T. Neuhaus, A. Schaffrath, D. Jerinić , "The pressure surge computer code DYVRO mod. 3: modelling and validation", The 13th International Topical Meeting on Nuclear Reactor Thermal-Hydraulics (NURETH-13), Kanazawa, Japan, September 27 - October 2, 2009.

[6] E. Altstadt, H. Carl, R. Weis, "Fluid-structure interaction experiments at the water-hammer test facility of Forschungszentrum Rossendorf", Jahrestagung Kerntechnik, Stuttgart, Germany, 14-16 May 2002, pp.559-564.

[7] A. Dudlik, S. B. H. Schoenfeld, O. Hagemann, H. Carl, H.-M. Prasser, "Water hammer and condensation hammer scenarios in power plants using new measurement system", The Practical Application of Surge Analysis for Design and Operation, 9th International Conference on Pressure Surges, Chester, UK, 24-26 March 2004, Vol. 1, pp. 151-165.

[8] H.-M. Prasser, Gy. Ezsöl, G. Baranyai, T. Sühnel, "Spontaneous water hammers in a steam line in case of cold water ingress", *Multiphase Science and Technology,* Vol. 20, No. 3-4, 2008, pp. 265-289.

[9] T. Neuhaus, A. Dudlik, "Experiments and comparing calculations on thermohydraulic pressure surges in pipes", The 11th International Topical Meeting on Nuclear Reactor

Thermal-Hydraulics (NURETH-11), Log Number: 540, Popes Palace Conference Center, Avignon, France, October 2-6, 2005.